

AD715791

Office of Naval Research
Contract N00014-67-A-0204-0027 NR 031-142

on

HIGH STRENGTH MATERIALS

**"Measurement and Interpretation of
Isothermal-Martensitic Kinetics"**

By

V. Raghavan and Morris Cohen

December 1970

This document has been approved
for public release and sale; its
distribution is unlimited.



TECHNICAL REPORT NO. 5

Reproduction in whole or in part is permitted for any purpose of the United States Government. Distribution of this document is unlimited.

Department of Metallurgy and Materials Science
Massachusetts Institute of Technology
Cambridge, Massachusetts 02139

Reproduced by
**NATIONAL TECHNICAL
INFORMATION SERVICE**
Springfield, Va. 22151

52

Security Classification

DOCUMENT CONTROL DATA - R & D

Security classification of title, body of abstract and indexing annotation must be entered when the overall report is classified

1. ORIGINATING ACTIVITY (Corporate method) Department of Metallurgy and Materials Science Massachusetts Institute of Technology Cambridge, Massachusetts		2a. SECURITY CLASSIFICATION Unclassified	
3. REPORT TITLE MEASUREMENT AND INTERPRETATION OF ISOTHERMAL-MARTENSITIC KINETICS		2b. GROUP	
4. DESCRIPTIVE NOTES (Type of report and, inclusive dates) Interim Technical Report			
5. AUTHOR(S) (First name, middle initial, last name) V. Raghavan and M. Cohen			
6. REPORT DATE December 1970	7a. TOTAL NO. OF PAGES 51	7b. NO. OF PAGES 31	
8a. CONTRACT OR GRANT NO. N00014-67-A-0204-0027 NR 031-142	9a. ORIGINATOR'S REPORT NUMBER(S) Technical Report No. 5		
b. PROJECT NO.	9b. OTHER REPORT NO(S) (Any other numbers that may be assigned this report)		
c.			
d.			
10. DISTRIBUTION STATEMENT Reproduction in whole or in part is permitted for any purpose of the United States Government. Distribution of this document is unlimited.			
11. SUPPLEMENTARY NOTES		12. SPONSORING MILITARY ACTIVITY Office of Naval Research	
13. ABSTRACT A brief survey of experimental work on isothermal martensitic transformations is given. Recent results on quantitative metallography are presented. Models for the isothermal kinetics and the method of evaluating the autocatalytic factor as well as the activation free energy for nucleation are discussed. The linear dependence of the activation energy on the chemical free-energy change is found to extrapolate satisfactorily to the low M_s temperatures exhibited by Fe-Ni alloys. The values obtained by substituting the above empirically-determined parameters into the Kaufman-Cohen nucleation equation indicate that the embryos in Fe-Ni alloys are more potent than those in Fe-Ni-Mn alloys, whereas the interfacial energies are quite similar.			

Unclassified

Security Classification

10 REF WORDS	LINK A		LINK B		LINK C	
	HOLE	WT	HOLE	WT	HOLE	WT
Nucleation; preferred nucleation sites; embryos; martensitic transformations; autocatalytic nucleation; quantitative metallography; iron-nickel alloys; iron-nickel-manganese alloys.						

DD FORM 1473 (BACK)
1 NOV 65
S/N 0102-014-6800

Unclassified

Security Classification

A-31409

MEASUREMENT AND INTERPRETATION OF ISOTHERMAL-MARTENSITIC KINETICS

V. Raghavan and Morris Cohen

A brief survey of experimental work on isothermal martensitic transformations is given. Recent results on quantitative metallography are presented. Models for the isothermal kinetics and the method of evaluating the autocatalytic factor as well as the activation free energy for nucleation are discussed. The linear dependence of the activation energy on the chemical free-energy change is found to extrapolate satisfactorily to the low M_s temperatures exhibited by Fe-Ni alloys. The values obtained by substituting the above empirically-determined parameters into the Kaufman-Cohen nucleation equation indicate that the embryos in Fe-Ni alloys are more potent than those in Fe-Ni-Mn alloys, whereas the interfacial energies are quite similar.

INTRODUCTION

Martensitic transformations in iron-base alloys have recently been classified according to the observed kinetic behavior. In one of the classifications⁽¹⁾, the transformations fall into three categories. The first of these is the well-known athermal transformation, where the progress of the reaction depends mainly on falling temperature. The second group includes certain Fe-Ni and Fe-Ni-C alloys with transformation ranges at subzero temperatures, where the reaction is initiated by an abrupt burst. Also, in this temperature range, we have the third category of completely-isothermal behavior, as exhibited by Fe-Ni-Mn and Fe-Ni-Cr alloys.

Another type of classification⁽²⁾ associates the athermal behavior with dynamic stabilization. In that context, the burst and the

completely-isothermal transformations are grouped together as "isothermal," the common feature between them being the absence of concurrent stabilization.

Based on recent findings, Raghavan and Cohen⁽³⁾ have redefined the transformation behavior at subzero temperatures in the following manner. They have now shown that a completely isothermal transformation to lenticular martensite occurs in an Fe - ~ 29Ni* alloy within a narrow temperature range, and this isothermal behavior is measurable from the very beginning of the transformation. On quenching the same alloy to still lower temperatures, however, transformation during cooling to the test temperature cannot be avoided, and the term "anisothermal" is adopted here to describe such reaction kinetics. The transformation under such conditions is thermally activated, but the activation energies for nucleation are then so low that the transformation rates cannot be measured experimentally. In the same Fe-Ni alloy, bursts with an audible click occur on quenching well into this range, with a substantial amount of martensite being formed in the order of microseconds^(4, 5). At still lower temperatures, the true athermal mode (i. e., transformation without thermal activation) prevails, at least in principle, and corresponds to the situation where the extrapolated activation energy for nucleation goes to zero.

In alloys containing more than 30 pct Ni, the initiation of the transformation with a burst is interpreted as an extreme form of autocatalysis, even though the transformation may still require some thermal activation⁽³⁾.

* Weight percentages are given throughout the text, unless otherwise indicated.

In the present paper, we are concerned with completely isothermal behavior and its interpretation on the basis of a nucleation model. The overall transformation kinetics is being treated elsewhere in this Symposium by A. R. Entwisle.

BRIEF SURVEY OF EXPERIMENTAL WORK ON ISOTHERMAL MARTENSITE

The isothermal mode of the martensitic transformation is now well documented^(1, 3, 6-19). Kurdjumov and Maksimova^(6, 7) were the first to report isothermal martensite in a number of steels and iron-base alloys. They found, for example, that in a 1.6 C steel, isothermal transformation occurs at temperatures below -100°C . Moreover, in a 0.6C - 6Mn - 2Cu steel⁽⁶⁾ and in an Fe - 23Ni - 3.4Mn alloy⁽⁷⁾, the isothermal transformation exhibits C-curve behavior. Both of these alloys can be quenched to -196°C without any transformation, but they start to transform on reheating. The maximum initial rate of transformation takes place around -130°C . The total quantity of isothermal martensite observed is also a maximum at this temperature.

Das Gupta and Lement⁽⁸⁾ noted that, in a 0.7C - 15Cr steel, isothermal transformation is always preceded by some athermal transformation and progresses by the formation of new lenticular plates rather than by the growth of existing ones.

Kulin and Speich⁽⁹⁾ studied the isothermal transformation in an Fe - 14Cr - 9Ni alloy, and showed that the transformation follows C-curve kinetics with a maximum rate at -35°C . The initial

martensite content at the start of the isothermal runs varied between 0 and 23 percent. The M_s in this alloy is dependent on the cooling rate; some martensite may be formed isothermally above the M_s^* .

Machlin and Cohen⁽¹⁰⁾ prequenched an Fe - 29Ni alloy into liquid nitrogen, before measuring the isothermal transformation at various higher holding temperatures. By this procedure, they were able to study the isothermal kinetics at a constant fraction of prior martensite. The isothermal rate had an interpolated maximum at -140°C . Recently, Anandaswaroop and Raghavan⁽¹¹⁾ employed a similar alloy and procedure to measure the isothermal nucleation rates upon reheating from a prequenching temperature of -95°C ; under these conditions, the maximum rate occurs at -70°C .

Cech and Hollomon⁽¹²⁾ reported on the isothermal transformation between -79 and -196°C in an Fe - 23Ni - 3.7Mn alloy. The transformation exhibited typical C-curve behavior, with the nose temperature at -130°C , thus confirming the findings of Kurdjumov and Maksimova⁽⁷⁾. At each holding temperature, the transformation rate was a maximum initially, and decreased as the reaction progressed. A surface layer of higher martensite content was formed to a depth of 0.002 to 0.005 inch during the isothermal transformation, and was attributed to the depletion of manganese or carbon from the surface during the austenitizing treatment.

Shih, Averbach and Cohen⁽¹³⁾ designed experiments to avoid the

* In the terminology adopted here, this type of reported M_s temperature is regarded as the beginning of the anisothermal transformation at the given cooling rate.

presence of surface martensite at the start of the isothermal run, and showed that (in the absence of any prior martensite) the initial isothermal transformation is quite slow compared to the accelerated rate observed as the reaction progresses. The reaction rate then decreases during the later stages of the transformation. Isothermal transformation curves typical of such behavior are shown in Fig. 1. However, the curves may be very different in shape if the transformation is determined after some martensite is formed by pre-quenching into liquid nitrogen. Due to the stimulating effect of the prior martensite, the subsequent isothermal transformation rate is a maximum initially and then decreases with time. Thus, it becomes clear that the basic characteristics of the isothermal reaction are best studied in the absence of any prior martensite, either at the surface or in the bulk. Recently, Entwisle⁽¹⁴⁾ and Pati and Cohen⁽¹⁵⁾ confirmed this significant point in a number of Fe-Ni-Mn alloys.

Philibert and Crussard⁽¹⁶⁾ found that, in a 1.4C - 2.5Cr steel, limited amounts of isothermal martensite may form after the regular cooling transformation. In addition, Philibert⁽¹⁷⁾ noted that if an Fe - 29Ni alloy is cooled step-by-step, each hold gives an isothermal curve with a transformation rate which is slow at first, and then increases with time before falling off again. He also showed that, if the carbon and nitrogen are sufficiently low, the burst character of the transformation disappears and isothermal mode occurs at higher temperatures.

In line with these results, Woodilla, Winchell and Cohen⁽¹⁸⁾ demonstrated that stabilization effects disappear on decarburization. Similarly, Yeo⁽¹⁹⁾ found that, in the presence of a strong carbide-forming element such as Ti, the stabilization due to carbon is absent, and then an Fe - 25Ni alloy can be isothermally transformed to over 90 pct of martensite.

Raghavan and Entwisle⁽¹⁾ investigated the isothermal transformation in an Fe - 26Ni - 2Mn alloy. Even though this alloy displays the isothermal mode over a wide range of temperatures (between -60 and -100° C), it could not be quenched into liquid nitrogen without the entré of a burst. Typical transformation curves at -66° C obtained with different austenitic grain sizes are plotted in Fig. 2. Their interpretation of this grain-size effect on the isothermal transformation is discussed in a later section.

Recently, Raghavan and Cohen⁽³⁾ measured the isothermal-transformation kinetics without prior martensite in two binary Fe-Ni alloys. Fig. 3 illustrates the isothermal transformation as a function of reaction temperature for an Fe - 29.2Ni - 0.21Mn - 0.006C alloy. The time to form 0.1 pct martensite (minimum detectable amount) is listed in Table I. The transformation is very sensitive to the test temperature, being barely detectable at -14.5° C and becoming too fast to measure isothermally below -22° C. Fig. 4 illustrates the microstructure obtained by isothermal transformation at -18° C; the morphology is

TABLE I

Time to Form the First Detectable Martensite ($t_{0.1}$) as a
Function of the Isothermal-Reaction Temperature, $T^{(3)}$

<u>$T, ^\circ\text{C}$</u>	<u>$t_{0.1}, \text{sec.}$</u>
-14.5	2400
-16.0	1200
-17.0	510
-18.0	162
-20.0	55
-22.0	27

clearly lenticular with some of the plates containing barely visible midribs. The midrib frequency in this alloy increases with decreasing reaction temperature, and becomes a significant feature of the microstructure at the lowest isothermal temperature (-22°C). Selected areas of the microstructure, often seen after isothermal transformation at -22°C , are shown in Fig. 5. The predominance of thick, midrib plates is evident. The boundaries between these plates are not well defined. Markings near the midrib region, identified earlier⁽²⁰⁾ as internal twins, are also observed.

Thick, midrib plates having more clearly defined boundaries, and showing twin markings near the midrib region with increasing frequency, begin to dominate the whole microstructure in specimens quenched a few degrees below -22°C . At these temperatures, the transformation is too rapid to measure isothermally. Whatever the crystallographic interpretation of these progressive changes may be, they take place without any apparent discontinuity in the kinetics. In other words, there is no abrupt kinetic transition corresponding to the increasing concentration of midrib plates in the microstructure.*

Fig. 6 indicates the isothermal transformation in an Fe - 28.8Ni - 0.002C alloy as a function of reaction temperature. This alloy transforms to nearly 60 pct of martensite at 0°C . As has been noted previously^(21, 22), the nickel content of this alloy is just about at the

* On quenching to still lower temperatures, this alloy begins to transform in a burst with an audible click.

transition between nonlenticular and lenticular morphology. Correspondingly, the microstructure in Fig. 7 exhibits a mixture of nonlenticular and lenticular martensite formed on isothermal transformation at 6° C. The nonlenticular martensite is of the lath (or packet) type, and is produced isothermally, as is the lenticular martensite, under these conditions.

QUANTITATIVE METALLOGRAPHIC MEASUREMENTS

Pati and Cohen⁽¹⁵⁾ employed quantitative metallographic techniques for measuring nucleation rates during isothermal martensitic transformations. At any given reaction temperature, they transformed a series of samples to various extents, and obtained the number of martensitic plates per unit test volume (N_v) in each specimen by Fullman's equation⁽²³⁾:

$$N_v = \frac{8 \bar{E} N_A}{\pi^2} \quad (1)$$

where N_A is the number of plates per unit area of random test plane, and \bar{E} is the mean reciprocal of the plate lengths as intersected by a random plane.

The mean volume of the plates \bar{v} up to any given stage of transformation is simply:

$$\bar{v} = f/N_v \quad (2)$$

where f is the volume fraction of martensite, and can be determined by point counting.

The nucleation rates are evaluated directly from these measurements. Fig. 8 is a plot of N_v as a function of transformation time for an Fe - 24Ni - 3Mn alloy reacted at -115°C . The nucleation rate at any instant is obtained from the slope of this plot:

$$\dot{N} = \frac{dN_v}{dt} \frac{1}{1-f} \quad (3)$$

It is evident that the nucleation rate increases appreciably during the initial part of the transformation (autocatalysis) and then decreases during the later stages. Pati and Cohen⁽²⁴⁾ also developed kinetic equations to generate the transformation curves, taking the autocatalytic effects into account as described in a later section.

SURFACE NUCLEATION

The importance of measuring the isothermal transformation in the absence of prior martensite, either at the surface or within the interior of the specimen, has already been stressed. Apart from the fact that surface martensite has morphological and crystallographic characteristics^(25, 26) different from those of bulk martensite, the fast nucleation rate at the surface interferes with the measurement of the slower volume nucleation during the early stages of transformation. The surface martensite tends to stimulate the bulk transformation by spreading inwards from the surface. Therefore, it is desirable to avoid surface nucleation for quantitative transformation studies in bulk samples.

The method currently used to achieve this end consists of enriching the outer layers of the specimen with a small amount of carbon, thus effectively stabilizing the surface against preferential nucleation. A suitable time-temperature combination is chosen for the final austenitizing treatment such that the right quantity of carbon is transferred to the specimen surface from a source.

Obviously, preferential surface nucleation can be caused by inadvertent decarburization, but the phenomenon is also associated with the free surface itself, e. g., the lack of three-dimensional constraint on the transformation shape-change at the surface. This condition can be offset, at least in part, by means of an electroplated layer which acts to constrain the surface, as described below.

Several samples of an Fe - 24Ni - 3Mn alloy were batch annealed at 900° C for 15 minutes in an argon atmosphere without a carbon source. One-half of these specimens were then transformed isothermally at -100° C, after electropolishing off the surface layers; special care was taken during all mechanical handling. Metallographic examination revealed these samples to have a greater concentration of martensite near the surface than in the interior. The other half of the samples were electropolished and then electroplated with a 0.001-inch thick adherent layer of nickel. None of these samples had any preferential concentration of martensite near the surface. By the same token, the transformation rates during the initial stages were always slower in

the plated specimens than in the unplated ones, as illustrated in Fig. 9. This finding is consistent with the deduction that preferential nucleation at the surface can enhance the overall transformation rate.

MODELS FOR ISOTHERMAL KINETICS

In the isothermal transformation, the increase in initial transformation rate is due to autocatalytic nucleation. The first martensitic plates produce more nucleation sites than they consume or sweep out, and this adds to the subsequent transformation rate. Direct measurements by quantitative metallography have clearly shown⁽¹⁵⁾ that the nucleation frequency increases with time during the early stages of isothermal transformation. The subsequent decrease in transformation rate is attributable to the partitioning effect, i. e., the volume fraction transformed per nucleation event progressively decreases, as the austenite is divided into smaller and smaller pockets.

Raghavan and Entwisle⁽¹⁾ took both these effects into account to give a quantitative interpretation of the isothermal martensitic kinetics. They proposed that the number of autocatalytic embryos generated is proportional to the volume fraction of martensite formed, and they adopted the partitioning model of Fisher et al.⁽²⁷⁾ to estimate the mean plate size as a function of fraction transformed. The transformation rate was taken to be the product of the nucleation rate and the volume fraction transformed per nucleation event, from which:

$$df/dt = (n_1 + pf - N_v)(1 - f) \nu \exp(-\Delta W_a/RT) m q (1 - f)^{1+1/m} \quad (4)*$$

* The $(1 - f)$ factor in Eq. (4) was omitted by Raghavan and Entwisle⁽¹⁾, but can be disregarded in the early stages of the transformation.

where f = the fraction of martensite formed,

t = time in seconds,

n_i = number of preexisting nucleation sites or embryos in the parent austenite (estimated as 10^7 per cm^3),

p = number of autocatalytic embryos produced per unit volume of martensite,

N_v = number of martensite plates per unit volume of alloy,

ν = lattice vibration frequency,

ΔW_a = activation energy for nucleation at temperature T ,

m = thickness-to-diameter ratio of the martensitic plates, and

q = average volume per grain of austenite.

The percentage of martensite as a function of time can be computed by numerical integration of Eq. (4). Both q and m are measured metallographically, and then the unknown quantities p and ΔW_a can be evaluated by curve-fitting the calculated to the experimental results. The curves thus computed agree quite well with the experimental data up to 8 - 10 pct transformation, as shown in Fig. 10 for an Fe - 26Ni - 2Mn alloy having a range of grain sizes. With further amounts of transformation, however, the derived curves fall below the experimental curves; this discrepancy will be discussed later.

The parameter m is known to vary as the transformation proceeds. For an Fe - 24Ni - 3Mn alloy, Pati and Cohen⁽¹⁵⁾ found that $1/m = 18 - 20f$ up to $f = 0.4$, but substituting this relationship into Eq. (4) results only in a minor improvement in the curve-fitting.

In order to make the above model more consistent with the experimental observation that plates often form in clusters during the early stages of transformation, Raghavan⁽²⁸⁾ considered a two-step process: (i) the increase with time of the number of austenitic grains in which first-plate nucleation takes place, and (ii) the progress of further transformation within such grains. Thus, the overall transformation rate becomes a function of both the spreading and filling-in processes which occur simultaneously. The outward spread of nucleation from a central grain due to autocatalysis is compared with the growth process in a typical nucleation and growth reaction. Following the Johnson-Mehl-Avrami treatment, an expression was obtained for the number of grains where first-plate nucleation has occurred (N_g):

$$N_g = 1/q [1 - \exp\{-qn_1\nu \exp(-\Delta W_a/RT)(2t^4/t'^3 + 4t^3/t'^2 + 3t^2/t' + t)\}] \quad (5)$$

where t' is the approximate time to nucleate the first plate in an austenitic grain which is stimulated from across its grain boundary.

Assuming that the autocatalytic effect is of the same magnitude on both sides of the grain boundary, and noting that the strained region around the first plate in a grain impinges on six neighboring grains, Raghavan⁽²⁸⁾ derived the following expression for t' :

$$t' \approx 1/\{(n_1q + mqp/6)\nu \exp(-\Delta W_a/RT)\} \quad (6)$$

where p is the same autocatalytic parameter that appears in Eq. (4).

The transformation rate within any one grain is then equal to:

$$df_g/dt = (n_i q + q p f_g - P)(1 - f_g) \exp(-\Delta W_a/RT) m (1 - f_g)^{1+1/m} \quad (7)$$

where f_g is the fraction of grain volume transformed, and P is the number of martensitic plates within the grain. Fisher's partitioning formula is adopted here, as in the earlier model.

Eq. (7) can be numerically integrated by taking sufficiently small time intervals to yield the desired accuracy. ΔN_g for such time intervals is obtained from Eq. (5), and then the increments of transformation from these grains in the first such time interval and in each subsequent one are successively added, keeping track of the progressive effects of partitioning in the different groups of grains.

The foregoing kinetic model⁽²⁸⁾, based on the cluster-formation of martensite, improves the agreement between the calculated and experimental curves, compared to the case in which the nonuniformity of embryo distribution arising from the autocatalytic process is not considered. In Fig. 11, the transformation curves calculated (A) by taking the cluster-formation sequence of plates into account, and (B) by assuming an uniform distribution of plates at all times, are plotted along with the experimental curve. Curve A matches the data up to 13 pct transformation. The disparity beyond this point has been shown by Pati and Cohen⁽²⁴⁾ to stem from the Fisher partitioning formula⁽²⁷⁾ which overestimates the number of martensitic plates required to give a certain fraction of transformation, especially beyond 20 pct martensite. This deduction is made possible

by introducing additional experimental data obtained from quantitative-metallographic measurements. The kinetic analysis is outlined below.

GENERATION OF TRANSFORMATION CURVES FROM METALLOGRAPHIC MEASUREMENTS

The mean volume per martensitic plate forming at any instant during isothermal transformation cannot be determined by direct measurements. On the other hand, it is quite feasible to obtain the mean volume (\bar{v}) per plate of all the plates present at any time. This is done by reacting a series of specimens to different amounts of martensite at a constant holding temperature, and then performing the metallographic measurements required by Eqs. (1) and (2). Such values of \bar{v} are summarized in Fig. 12 for an Fe - 24Ni - 3Mn alloy transformed at various reaction temperatures both above and below the nose of the C-curve (-125° C). These results are surprising in that the mean volume of the martensitic plates depends not only on the extent of transformation (partitioning), but also on the reaction temperature. Evidently, partitioning is not just a problem of spatial geometry.

More recently, Pati and Cohen⁽²⁴⁾ have attempted to avoid any reliance on a partitioning relationship by incorporating the actual \bar{v} -determinations (Fig. 12) in the kinetic treatment. The number of most-potent embryos (n_t) existing at any time per unit volume of alloy is taken, as previously⁽¹⁵⁾:

$$\begin{aligned} n_t &= (n_i + pf - N_v)(1 - f) \\ &= (n_i + f [p - 1/\bar{v}])(1 - f) \end{aligned} \quad (8)$$

and rate of activation of such embryos per unit volume of alloy is:

$$d N_v / dt = n_t \nu \exp (-\Delta W_a / RT) \quad (9)$$

The isothermal transformation rate is simply:

$$\frac{df}{dt} = \frac{dN_v}{dt} \cdot v \quad (10)$$

where v is the volume per martensitic plate formed at time t . In the previous kinetic Eqs. (4) and (7), v has been expressed through the Fisher partitioning formula⁽²⁷⁾. Instead, we now note from

Eq. (2) that:

$$\begin{aligned} \frac{df}{dt} &= \bar{v} \frac{dN_v}{dt} + N_v \frac{d\bar{v}}{dt} \\ &= \frac{dN_v}{dt} \left(\bar{v} + N_v \frac{d\bar{v}}{dN_v} \right) \end{aligned} \quad (11)$$

and by comparing Eqs. (10) and (11), we see that:

$$v = \bar{v} + N_v \frac{d\bar{v}}{dN_v} \quad (12)$$

Inasmuch as all the quantities on the righthand side of Eq. (12) can be obtained by quantitative metallography⁽²⁴⁾, the Fisher partitioning assumption can be replaced by experimental quantities, and then:

$$\frac{df}{dt} = (n_i + f [p - 1/\bar{v}]) (1 - f) \nu \exp (-\Delta W_a / RT) \left(\bar{v} + N_v \frac{d\bar{v}}{dN_v} \right) \quad (13)$$

For each reaction temperature, \bar{v} is known as a function of f from Fig. 12, and then N_v can be obtained as a function of f through Eq. (2). Accordingly, the derivative $d\bar{v}/dN_v$ in Eq. (11) can also be evaluated, leaving p and ΔW_a as the only two adjustable parameters. Using the

same curve-fitting procedure as before to fix these parameters for each reaction temperature, Pati and Cohen⁽²⁴⁾ obtained the results plotted in Figs. 13, 14 and 15 for the entire range of isothermal transformations in their Fe - 24Ni - 3Mn alloy.

These findings emphasize that the previously adopted partitioning formula becomes highly inaccurate as the transformation proceeds. Although Fig. 12 indicates that partitioning does occur, the extent depends on the reaction temperature (i. e. , the temperature-dependent morphology plays a significant role), and the plate sizes do not change by orders of magnitude as required by the Fisher formula.

A time-normalized* plot of the initial stages of the transformation curves (Figs. 13-15) is illustrated in Fig. 16. The curvature of these normalized curves passes through a maximum near the nose of the C-curve, because the curvature depends on the factor $[p - 1/\bar{v}]$ in Eq. (11). This interesting behavior arises mainly because of the variations in \bar{v} , as just discussed. The autocatalytic factor p is found to be relatively insensitive to temperature over this range⁽²⁴⁾.

GRAIN-SIZE EFFECTS

Fig. 2 demonstrates that the rate of isothermal transformation increases with the austenitic grain size⁽¹⁾. This is the case even when the final austenitizing temperature is held constant.

The autocatalytic parameter p , as obtained from Eq. (4) through

* The time scale is normalized for present purposes by dividing the actual reaction time (t) by the time ($t_{1,0}$) for 1 pct transformation.

curve-fitting, is found to be independent of the grain size⁽¹⁾. However, \bar{v} at any given stage of transformation (f) is larger, the larger the grain size. This is true whether the martensitic plates extend entirely across the austenitic grains⁽¹⁾ or not⁽¹⁵⁾. The factor $[p - 1/\bar{v}]$ in Eq. (13) is usually positive, and controls the observed acceleration of the transformation due to autocatalysis. Under such conditions, then, the autocatalytic effect is greater, i. e. $[p - 1/\bar{v}]$ is larger, when the grain size is larger.

Pati and Cohen⁽¹⁵⁾ also showed that the autocatalytic acceleration of the isothermal transformation can be eliminated by adjusting the grain size and transformation conditions to make $[p - 1/\bar{v}] \approx 0$. This means that the generation of new embryos during the reaction is just counterbalanced by the consumption of embryos, and the number of embryos per unit untransformed volume ($\frac{n_t}{1-f}$) in Eq. (8) remains substantially constant at n_i . If $[p - 1/\bar{v}]$ happens to be negative, the number of embryos per unit untransformed volume becomes smaller with time, and the nucleation rate then decreases monotonically, causing the transformation to come to a halt.

ACTIVATION-ENERGY CALCULATIONS

In deriving the activation energy for the isothermal nucleation of martensite, Shih et al.⁽¹³⁾ estimated an initial embryo concentration of one per grain, which gave $n_i = 10^5$ per cm^3 for the austenitic grain size in their experiments. Assuming a constant rate of nucleation up

to the first detectable amount of martensite (0.2 pct), they then calculated the activation energies from the following equations:

$$\dot{N} = n_i \nu \exp (-\Delta W_a / RT) \quad (14)$$

$$0.002 = \dot{N} v_i \tau_i \quad (15)$$

where v_i is the volume of the first plates to form, and τ_i is the time to produce 0.2 pct martensite.

Raghavan and Entwisle⁽¹⁾ took n_i to be 10^7 per cm^3 . They noted that the transformation curves must be nonlinear even up to 0.2 pct transformation, and made allowance for this on the basis of autocatalysis. They also assumed, as did Shih et al.⁽¹³⁾, that the initial plates were stopped only by grain and twin boundaries.

Pati and Cohen⁽¹⁵⁾ refined the activation-energy calculations further, avoiding the assumption that the plate size is controlled by grain-boundary or twin-boundary barriers, and employing quantitative metallography for a more direct measurement of v_i . They also took into account the increase in the nucleation rate due to autocatalysis, as proposed by Raghavan and Entwisle⁽¹⁾. The results for an Fe-24Ni-3Mn alloy are given in Table II. The activation energies lie in the range of 5,000 - 15,000 cal/mole, and decrease monotonically with decreasing reaction temperature. These values differ by less than 10 pct from those previously published^(1, 13).

ACTIVATION-ENERGY DEPENDENCE ON DRIVING FORCE

The activation energies for isothermal-martensitic nucleation in

TABLE II

Activation Energies for Initial Martensitic

Nucleation in an Fe - 24Ni - 3Mn Alloy⁽¹⁵⁾

Reaction Temperature °C	ΔW_a cal/mole
- 70	15,600
- 80	13,800
- 90	12,600
-105	11,500
-115	10,600
-125	9,800
-140	8,800
-150	8,200
-183	6,400
-196	5,800

Fe-Ni-Mn alloys is linearly related to the chemical driving force of the transformation. This is indicated in Fig. 17, the empirical relationship being:

$$\Delta W_a = 1.05 \times 10^{-21} (\Delta g) + 3.66 \times 10^{-12} \text{ ergs/event} \quad (16)$$

In the case of the Fe-29.2Ni alloy (with lenticular morphology), the equation is:

$$\Delta W_a = 3.69 \times 10^{-21} (\Delta g) + 8.27 \times 10^{-12} \text{ ergs/event} \quad (17)$$

These linear relationships are consistent with the Kaufman-Cohen model for isothermal nucleation of preexisting embryos^(30, 31).

Using the values of the slope and intercept from Eq. (17) and the free-energy data for Fe-Ni alloys, Raghavan and Cohen⁽³⁾ have calculated the time for the initial 0.1 percent transformation ($t_{0.1}$) as a function of nickel content and reaction temperature, as shown in Fig. 18. Only nickel contents above 29 pct Ni are considered here because lenticular morphologies are not commonly found at lower nickel levels in Fe-Ni alloys^(21, 22).

For comparison with experimental M_s data, the transformation-start temperatures at any given cooling rate can be estimated from Fig. 18 as follows. The fractional times ($\Delta t/t_{0.1}$) that the specimen spends at successive 1° C temperature intervals are added. The temperature at which this integrated time becomes unity is then taken

as the anisothermal M_s . For a cooling rate of 5°C/min. , $\Delta t = 0.2$ min. and the anisothermal M_s turns out to be the temperature at which $t_{0.1} \approx 0.5$ min. The values thus obtained are compared in Table III with those determined experimentally⁽²⁹⁾ at the same cooling rate. The calculated anisothermal M_s temperatures agree reasonably well with the experimental values, disappearing at exactly the same nickel content (33 a/o Ni).

Table III also lists the athermal M_s temperatures where ΔW_a goes to zero, thus giving the insuppressible M_s . Of course, the athermal M_s lies below the anisothermal M_s , the latter being dependent on the cooling rate. Due to limitations in the cooling rate that can be achieved in practice, the anisothermal M_s becomes virtually insuppressible when ΔW_a is sufficiently small, even though the athermal M_s where $\Delta W_a = 0$ is not actually reached.

These calculations also indicate a measurable isothermal transformation range of about 10°C at 29 a/o Ni decreasing to 6°C at 33 a/o Ni, as defined by the vertical dashed lines in Fig. 18. Yet, such an isothermal range has not been found in alloys with more than 29 a/o Ni. Instead, the transformation seems to set in abruptly in the higher-nickel alloys. As pointed out by Magee⁽²⁾, a strong autocatalytic activity may be obscuring the isothermal transformation in the latter alloys.

It is interesting to note that only a three-fold increase in the slope and intercept terms of Eqs. (16) and (17) is sufficient to change the

TABLE III
Calculated M_s Temperatures for Fe-Ni Alloys
Compared with (Normalized) Experimental Values

Atomic % Ni	Normalized Experimental M_s , °K	Anisothermal M_s , °K (Cooling Rate 5° C/min)	Athermal M_s , °K ($\Delta W_a = 0$)
28.4	252	252	202
29.3	226	225	178
29.7	214	211	166
30.7	184	170	130
30.9	177	161	122
31.7	141	123	90
32.4	110	82	56
32.7	76	60	38
33.0	33	30	16
33.2	-	-	-
33.4	-	-	-

predominantly isothermal C-curve kinetics of Fe-Ni-Mn alloys⁽¹³⁾ to the essentially athermal kinetics of Fe-Ni alloys⁽²⁹⁾.

ISOTHERMAL NUCLEATION AND THE KAUFMAN-COHEN MODEL

The Kaufman-Cohen model^(30, 31) of an oblate-spheroidal embryo assumes slip as the lattice-invariant shear, whereas internal twinning is operative for the lattice-invariant shear in the present alloys, at least in the early stages of plate formation. However, no model is available which incorporates twinning in the nucleation energetics, and so we adopt the Kaufman-Cohen model for our purposes. In this model, the driving stress on the interface must not only overcome the restraining stress arising from the surface-energy and strain-energy terms, but must also provide for the athermal creation of new dislocation loops at the tips of the embryos. When this excess stress is not quite sufficient in magnitude, thermal fluctuations can bridge the gap. The resulting relationship between activation energy for isothermal nucleation (ΔW_a) and the chemical driving force (Δg) turns out to be:

$$\Delta W_a = 4 \times 10^{-2} \left(\frac{\sigma}{A} \right)^{1/2} (3\sigma r_e^{3/2} + \Delta g \left(\frac{\sigma}{A} \right)^{1/2} r_e^2) \text{ ergs/event} \quad (18)$$

Note that ΔW_a is linearly dependent on Δg , in line with the experimental relationships in Eqs. (16) and (17). The strain-energy parameter (A) is usually taken as 2.1×10^{10} ergs/cm³. Eqs. (17) and (18) then give 420 Å for the embryo radius (r_e) in the Fe-Ni alloys and 110 ergs/cm² for the interfacial energy (σ). The corresponding values for the

Fe-Ni-Mn alloys are 220 \AA and 120 ergs/cm^2 respectively. Since r_e is probably a measure of the embryo potency rather than its actual size, we see that manganese reduces the embryo potency when added to Fe-Ni alloys.

An attempt is now underway to adapt the above nucleation model to the case of a twin-dislocation interface instead of a dislocation-loop interface^(30, 31), thus simulating the internally-twinned martensites involved in these isothermal transformations of Fe-Ni and Fe-Ni-Mn alloys. The preliminary indications are that the above values for the embryo sizes and interfacial energies will not be changed in order of magnitude by these further refinements in the calculations.

CONCLUSIONS

1. Isothermal martensitic transformations in the bulk can be affected by preferential surface nucleation. Accordingly, the latter must be avoided in order to measure nucleation kinetics characteristic of the volume.
2. The isothermal transformation rate increases initially due to autocatalysis, whereas the subsequent decrease in the transformation rate can be attributed to the partitioning of the untransformed phase.
3. The usual partitioning formula seriously underestimates the mean plate volume at martensite fractions greater than 0.15.
4. The computed transformation curves generated by feeding-in quantitative metallographic data show satisfactory overall agreement with the experimental curves. This is not the case when the usual

partitioning formula is assumed.

5. The activation free energy for isothermal nucleation is linearly dependent on the chemical free-energy change of the austenite \rightarrow martensite transformation. The slopes and the intercepts of the linear equations are significantly different between Fe-Ni-Mn on the one hand and Fe-Ni alloys on the other. This difference is sufficient to change the predominantly isothermal C-curve kinetics in Fe-Ni-Mn alloys to the essentially athermal kinetics in the Fe-Ni alloys.

6. Substitution of the empirically-determined parameters into the Kaufman-Cohen equation for isothermal nucleation of preexisting embryos indicate that the embryos in Fe-Ni alloys are more potent than those in Fe-Ni-Mn alloys.

ACKNOWLEDGMENTS

This work was carried out as a part of a research program at MIT sponsored by the Office of Naval Research. Very helpful discussions were held with Drs. L. Kaufman and S. R. Pati.

REFERENCES

1. V. Raghavan and A. R. Entwisle: Iron and Steel Institute Special Report No. 93, 1965, p. 30.
2. C. L. Magee: Phase Transformations, p. 115, ASM, 1970.
3. V. Raghavan and M. Cohen: to be published.
4. R. F. Bunshah and R. F. Mehl: Trans. TMS-AIME, 1953, vol. 197, p. 1251.

5. K. Mukherjee: Trans. TMS-AIME, 1968, vol. 242, p. 1495.
6. G. V. Kurdjumov and O. P. Maksimova: Doklady Akademii Nauk SSR, 1948, vol. 61, no. 1, p. 83.
7. G. V. Kurdjumov and O. P. Maksimova: Doklady Akademii Nauk SSR, 1950, vol. 73, no. 1, p. 95.
8. S. C. Das Gupta and B. S. Lement: Trans. TMS-AIME, 1951, vol. 191, p. 727.
9. S. A. Kulin and G. R. Speich: Trans. TMS-AIME, 1952, vol. 194, p. 258.
10. E. S. Machlin and M. Cohen: Trans. TMS-AIME, 1952, vol. 194, p. 489.
11. A. V. Anandaswaroop and V. Raghavan: Scripta Met., 1969, vol. 3, p. 221.
12. R. E. Cech and J. H. Hollomon: Trans. TMS-AIME, 1953, vol. 197, p. 685.
13. C. H. Shih, B. L. Averbach and M. Cohen: Trans. TMS-AIME, 1955, vol. 203, p. 183.
14. A. R. Entwisle: Metal Sci. J., 1968, vol. 2, p. 153.
15. S. R. Pati and M. Cohen: Acta Met., 1969, vol. 17, p. 189.
16. J. Philibert and C. Crussard: J.I.S.I., 1955, vol. 180, p. 39.
17. J. Philibert: I.R.S.I.D. Serie, 1956, vol. A139, p. 55.
18. J. Woodilla, P. G. Winchell and M. Cohen: Trans. TMS-AIME, 1958, vol. 215, p. 849.

19. R. B. G. Yeo: Trans. TMS-AIME, 1962, vol. 224, p. 1222.
20. R. L. Patterson and C. M. Wayman: Acta Met., 1966, vol. 14, p. 347.
21. W. S. Owen, E. A. Wilson and T. Bell: High Strength Materials, p. 167, John Wiley, 1965.
22. V. V. Nemirovskiy: Phys. Metals. Metallog., 1968, vol. 25, no. 5, p. 141.
23. R. L. Fullman: Trans. TMS-AIME, 1953, vol. 197, p. 447.
24. S. R. Pati and M. Cohen: to be published.
25. J. A. Klostermann and W. G. Burgers: Acta Met., 1964, vol. 12, p. 355.
26. T. Homma: J. Jap. Inst. Metals, 1957, vol. 21, p. 126.
27. J. C. Fisher, J. H. Hollomon and D. Turnbull: Trans. TMS-AIME, 1949, vol. 185, p. 691.
28. V. Raghavan: Acta Met., 1969, vol. 17, p. 1299.
29. L. Kaufman and M. Cohen: Trans. TMS-AIME, 1956, vol. 206, p. 1393.
30. L. Kaufman and M. Cohen: Prog. Met. Phys., 1958, vol. 7, p. 165.
31. M. Cohen: Trans. TMS-AIME, 1958, vol. 212, p. 171.

FIGURE CAPTIONS

Figure Number

- 1 Isothermal transformation curves for Fe-23Ni-3.6Mn alloy at indicated temperatures for samples containing no initial martensite. Insert figure shows the early transformation⁽¹³⁾.
- 2 Isothermal transformation curves at -66° C for Fe-26Ni-2Mn alloy as a function of grain size. Grain diameters (mm) are indicated on curves⁽¹⁾.
- 3 Isothermal transformation curves for Fe-29.2Ni-0.2Mn alloy at indicated temperatures for samples containing no initial martensite⁽³⁾.
- 4 Microstructure obtained by isothermal transformation at -18° C of Fe-29.2Ni-0.2Mn alloy⁽³⁾.
- 5 Selected area in the microstructure obtained by isothermal transformation at -22° C of Fe-29.2Ni-0.2Mn alloy. The predominance of thick, midrib plates is evident⁽³⁾.
- 6 Isothermal transformation curves for Fe-28.8Ni alloy at indicated temperatures⁽³⁾.
- 7 Microstructure obtained by isothermal transformation at 6° C of Fe-28.8Ni alloy, showing both lenticular and non-lenticular morphologies. Arrows indicate surfacetilts due to spontaneous transformation on the electropolished

surface⁽³⁾.

- 8 Number of martensitic plates formed per unit test volume (N_v), as a function of transformation time at -115°C in Fe-24Ni-3Mn alloy⁽²⁴⁾.
- 9 Effect of nickel plating on isothermal martensitic transformation at -100°C .
- 10 Comparison of experimental transformation curves with those computed from Eq. (4) for Fe-26Ni-2Mn alloy transformed at -66°C . Grain diameters (mm) are indicated on curves⁽¹⁾.
- 11 Transformation curves for Fe-26Ni-2Mn alloy calculated (a) by taking the formation sequence of plates into account, and (b) by assuming a uniform distribution of plates at all times, compared with the experimental curve⁽²³⁾.
- 12 Mean plate volume (\bar{v}) as a function of martensitic fraction (f) at indicated temperatures⁽²⁴⁾.
- 13-15 Comparison of experimental transformation curves (Fe-24Ni-3Mn alloy) with those computed from quantitative metallographic data⁽²⁴⁾.
- 16 Time-normalized transformation curves for (Fe-24Ni-3Mn alloy) showing the initial stages of the transformation at the indicated temperatures.

- 17 Measured activation energies for the isothermal martensitic transformation in Fe-Ni-Mn alloys as a function of free-energy change accompanying the transformation⁽¹⁵⁾.
- 18 Time for the initial 0.1 pct transformation ($t_{0.1}$) as a function of temperature and nickel content⁽³⁾.

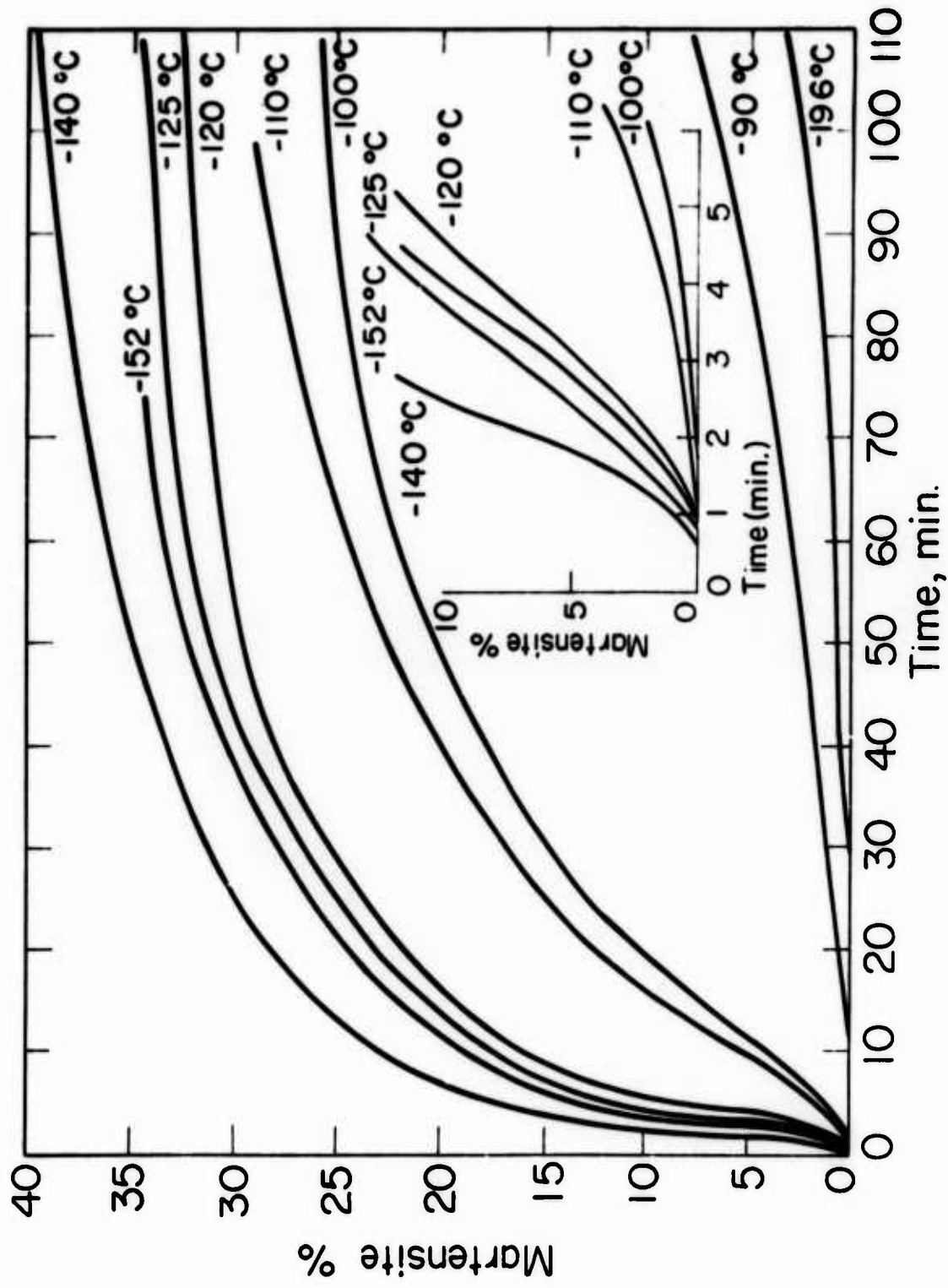


Fig.1 Isothermal transformation curves for Fe-23Ni-3.6Mn alloy at indicated temperatures for samples containing no initial martensite. Insert figure shows the early transformation⁽¹³⁾.

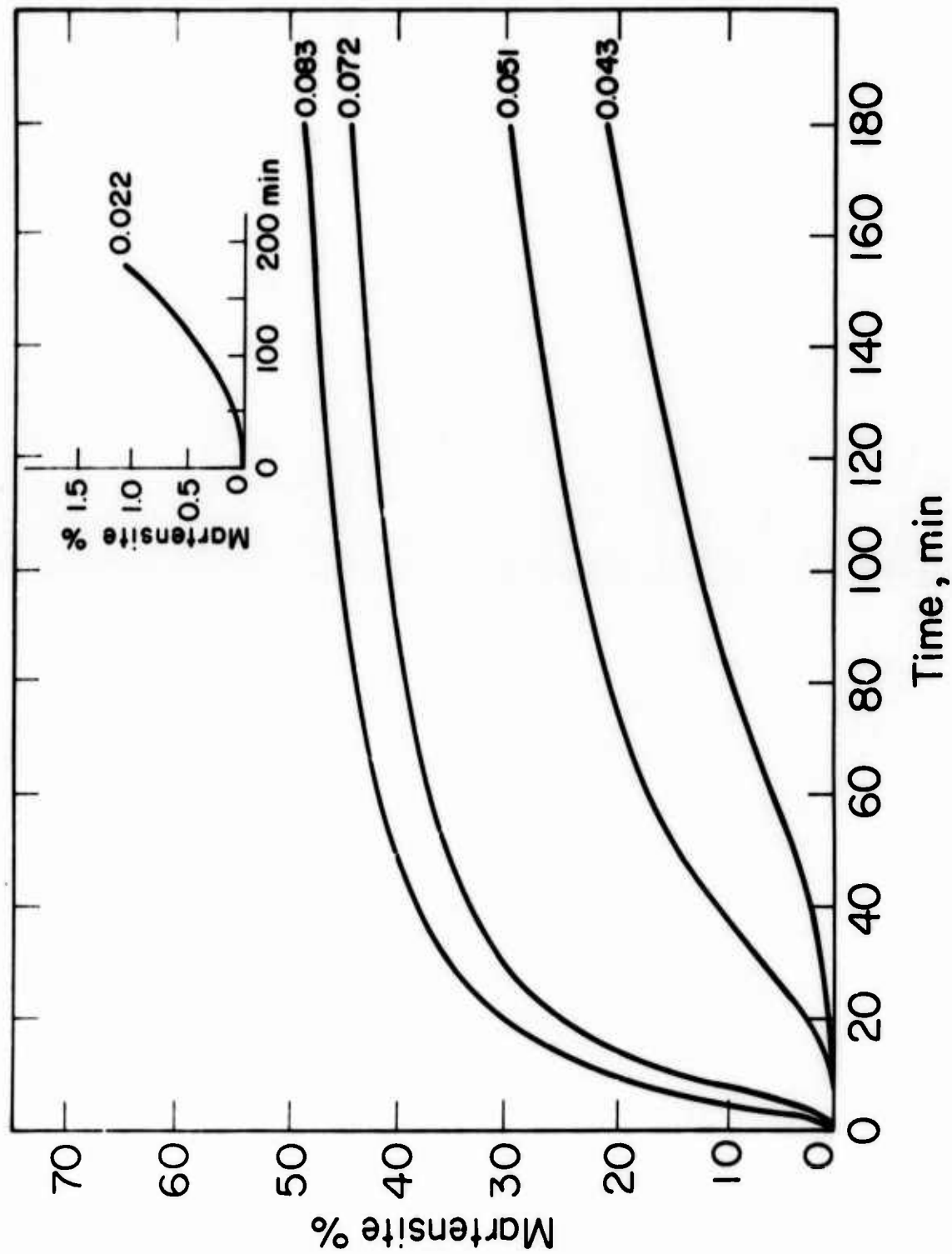


Fig. 2 Isothermal transformation curves at -66°C for Fe-26 Ni-2 Mn alloy as a function of grain size. Grain diameters (mm) are indicated on curves⁽¹⁾.

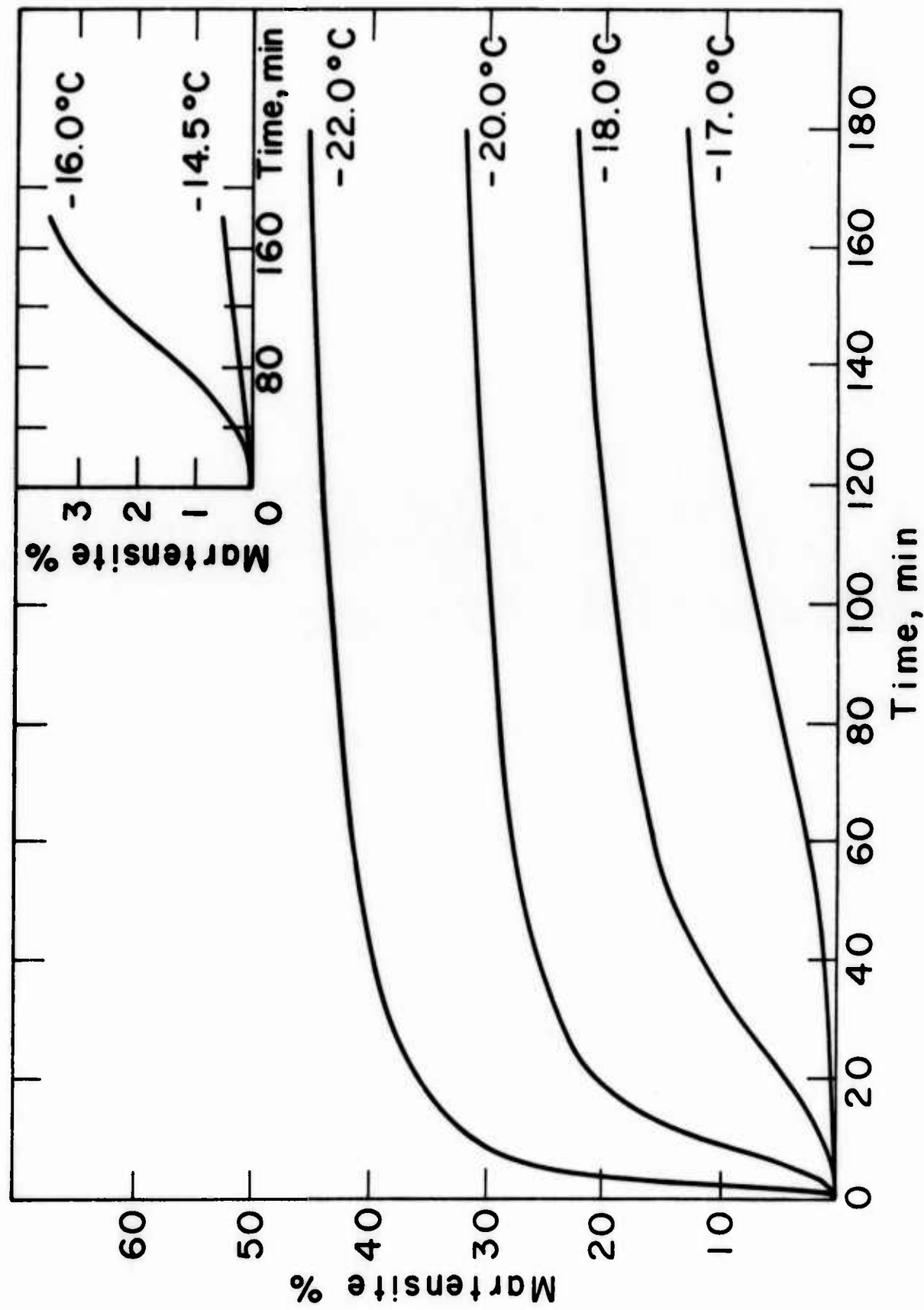


Fig. 3 Isothermal transformation curves for Fe-29.2Ni-0.2Mn alloy at indicated temperatures for samples containing no initial martensite⁽³⁾.



Fig. 4 Microstructure obtained by isothermal transformation at -18°C of Fe- 29.2 Ni - 0.2 Mn alloy⁽³⁾.



Fig. 5 Selected area in the microstructure obtained by isothermal transformation at -22°C of Fe-29.2Ni-0.2Mn alloy. The predominance of thick, midrib plates is evident(3).

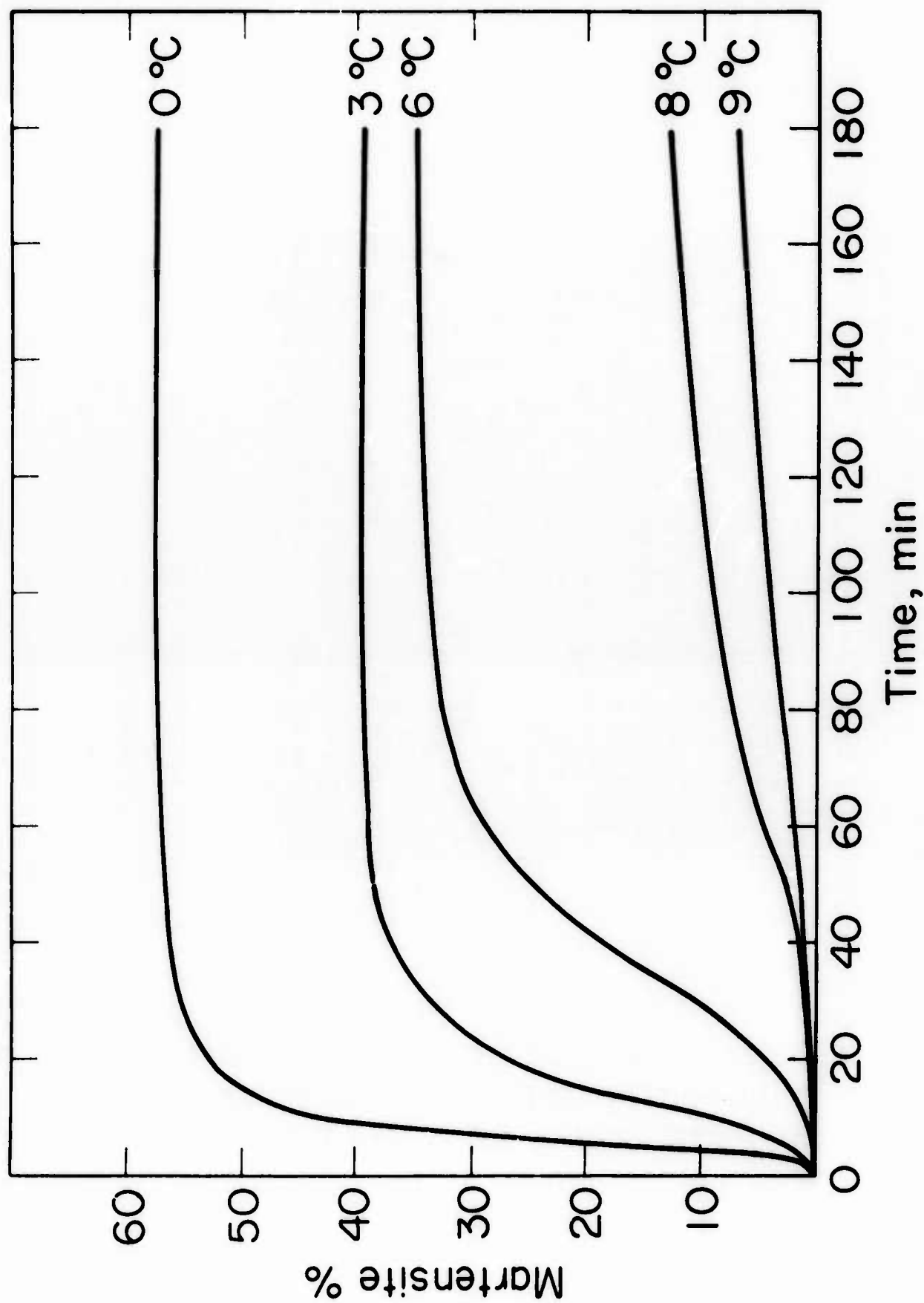


Fig. 6 Isothermal transformation curves for Fe- 28.8 Ni alloy at indicated temperatures⁽³⁾.

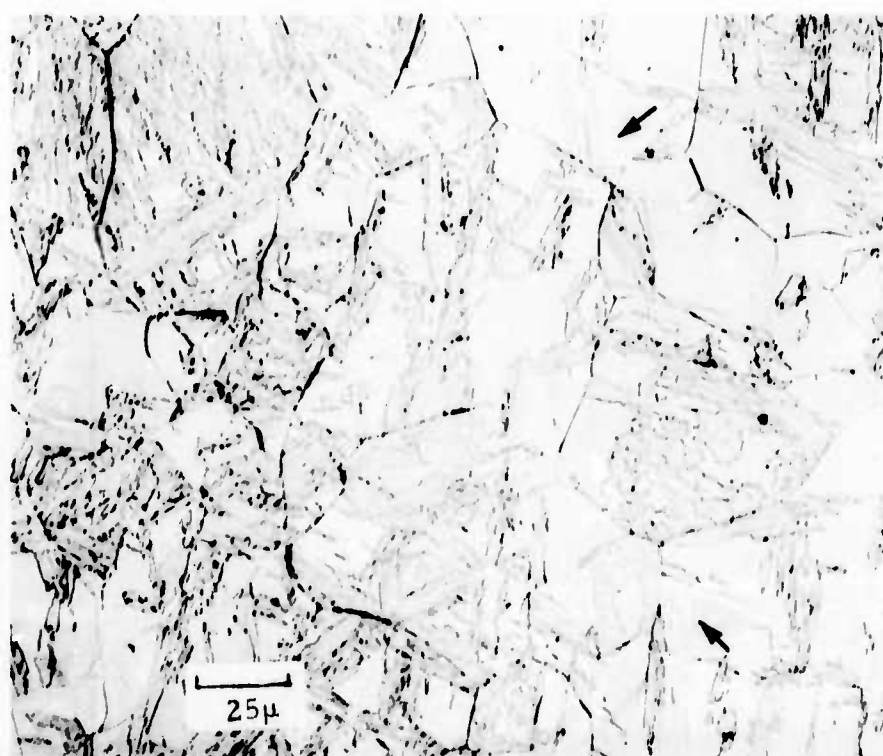


Fig. 7 Microstructure obtained by isothermal transformation at $+6^{\circ}\text{C}$ of Fe - 28.8 Ni alloy, showing both lenticular and nonlenticular morphologies. Arrows indicate surface tilts due^{to} spontaneous transformation on the electropolished surface(3).

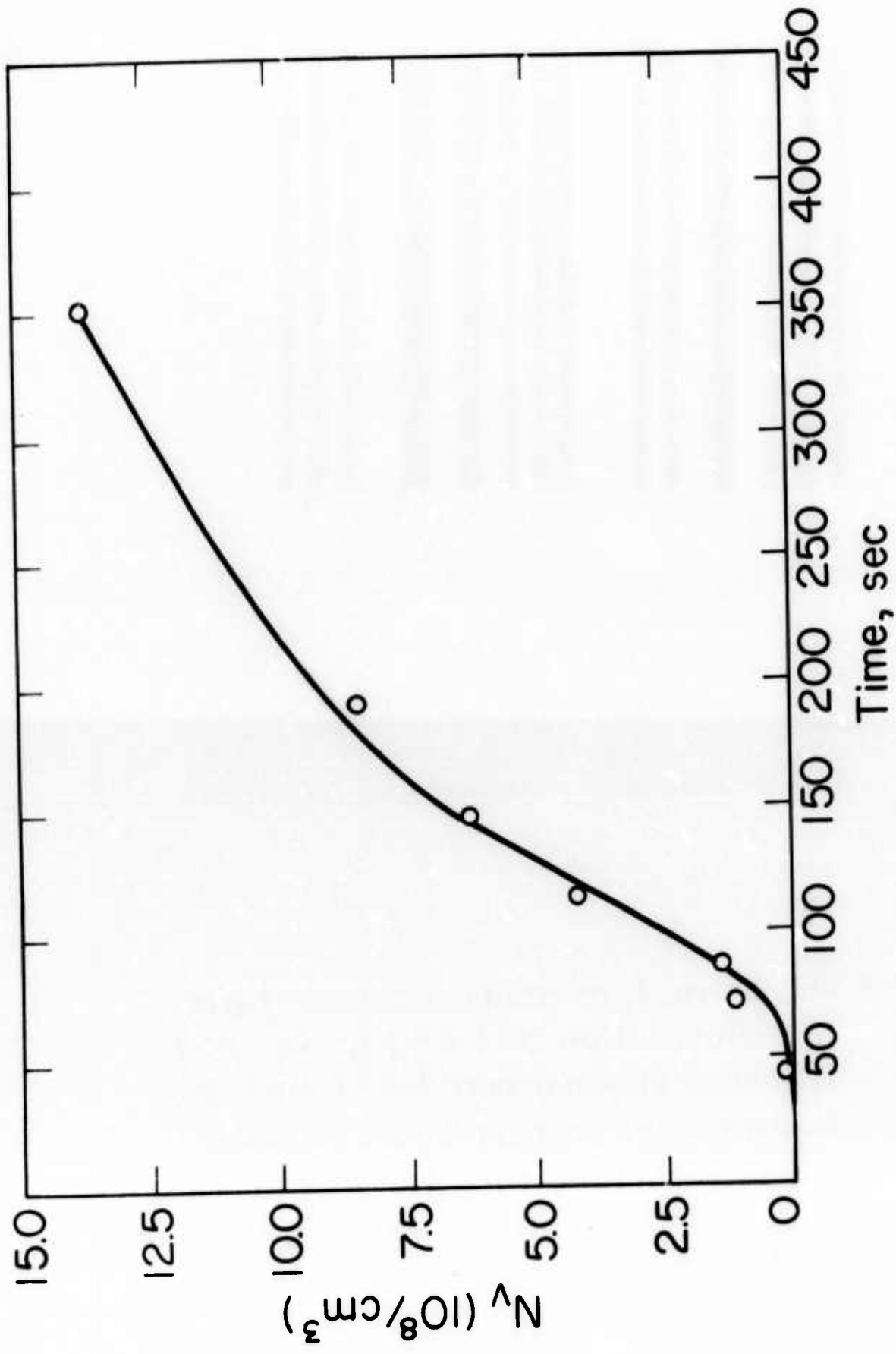


Fig. 8 Number of martensitic plates formed per unit test volume (N_v) as a function of transformation time at -115°C in Fe-24 Ni - 3 Mn alloy (24)

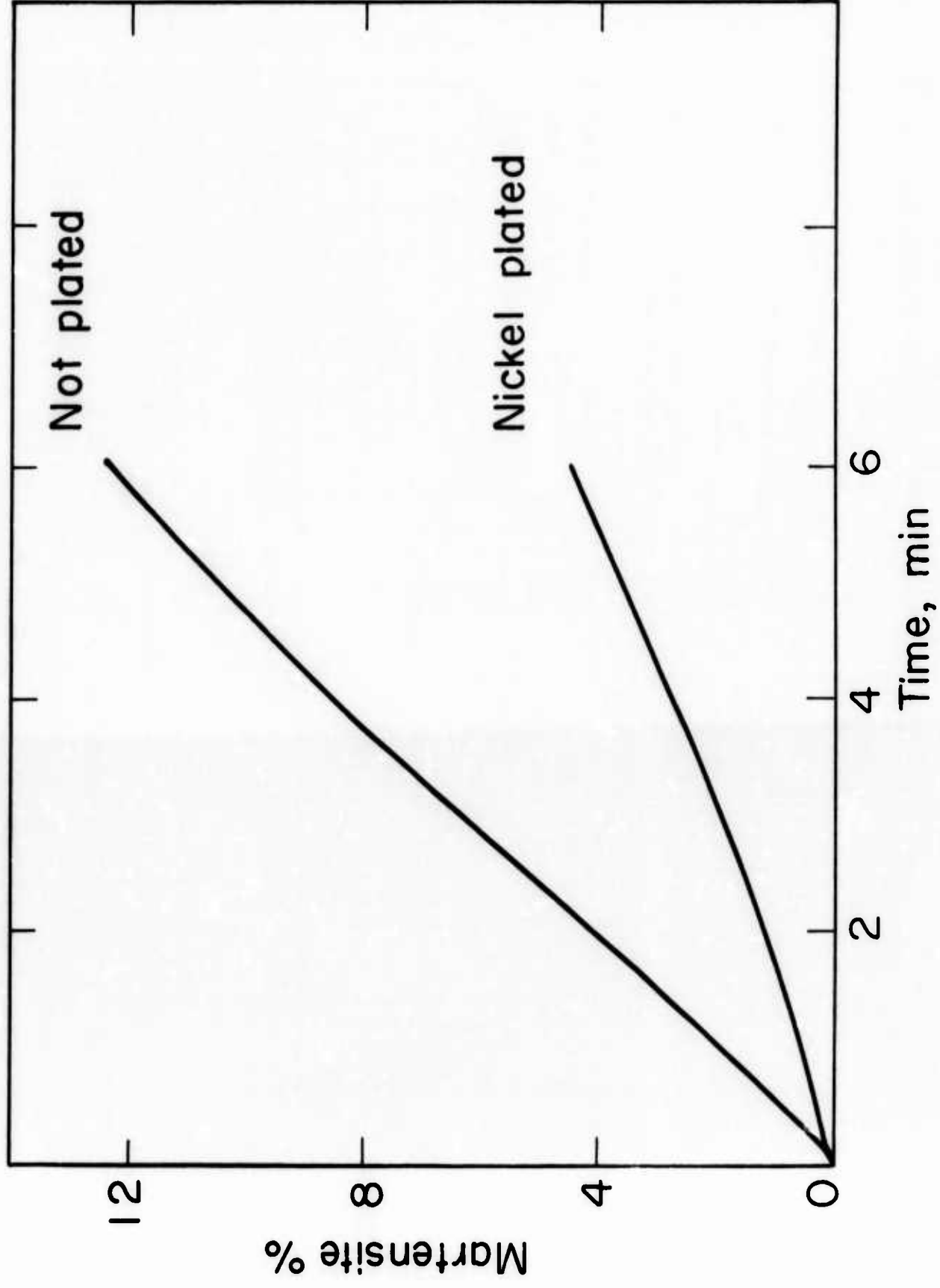


Fig. 9 Effect of nickel plating on isothermal martensitic transformation at -100°C .

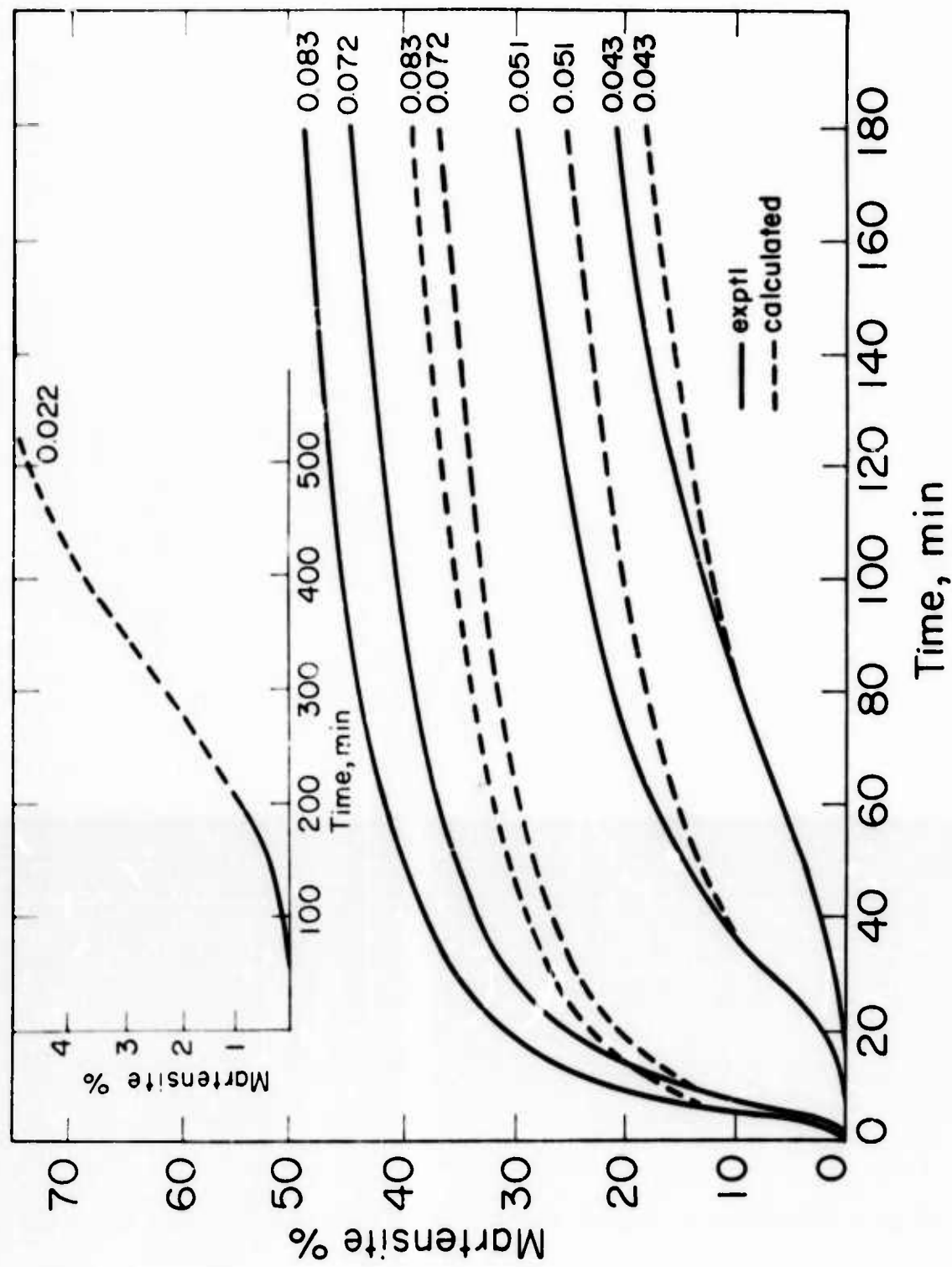


Fig. 10 Comparison of experimental transformation curves with those computed from equation (4) for Fe-26Ni 2 Mn alloy transformed at -66°C. Grain diameters (mm) are indicated on curves(1).

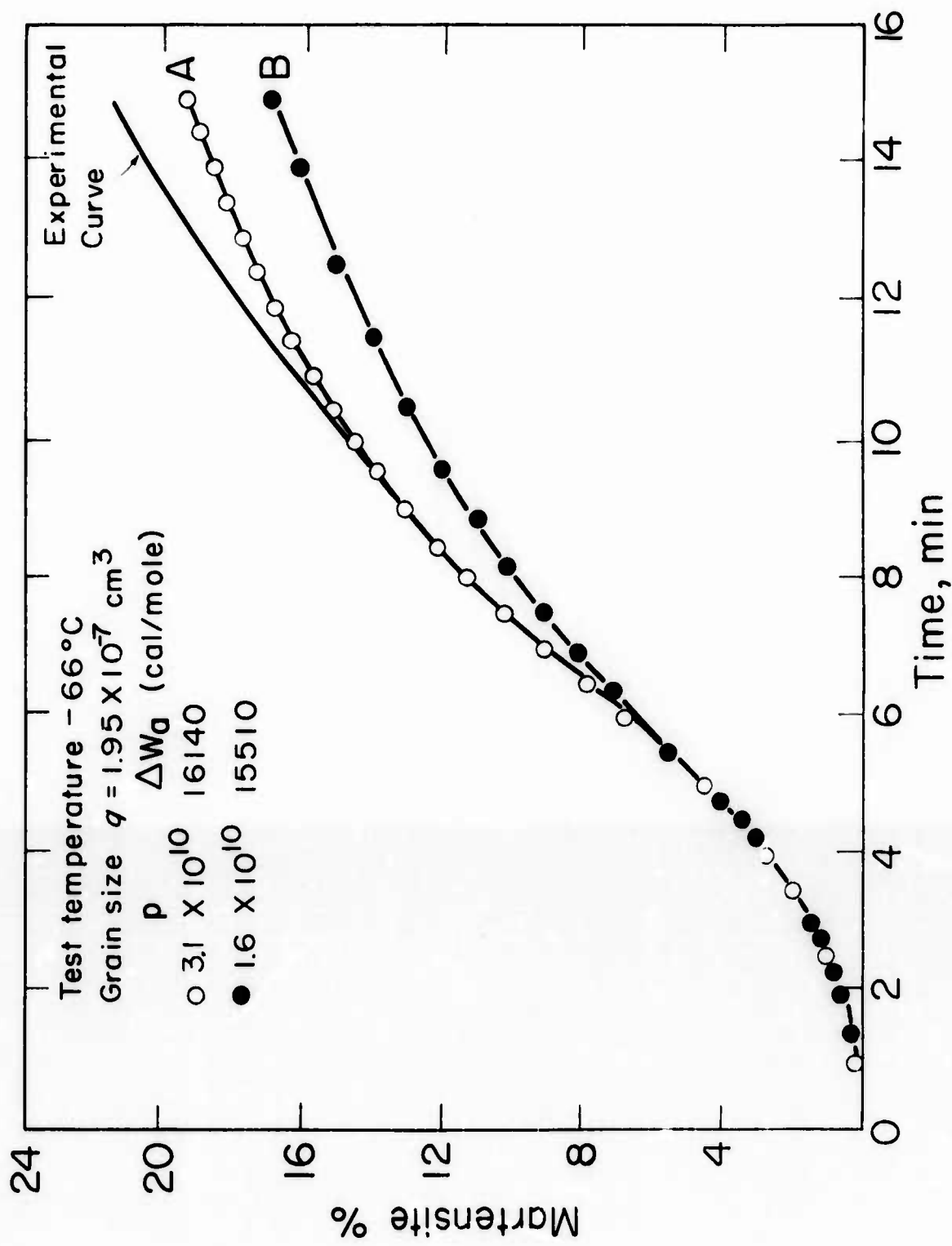


Fig. 11 Transformation curves for Fe-26Ni-2Mn alloy calculated (a) by taking the formation sequence of plates into account, and (b) by assuming a uniform distribution of plates at all times, compared with experimental curve (28).

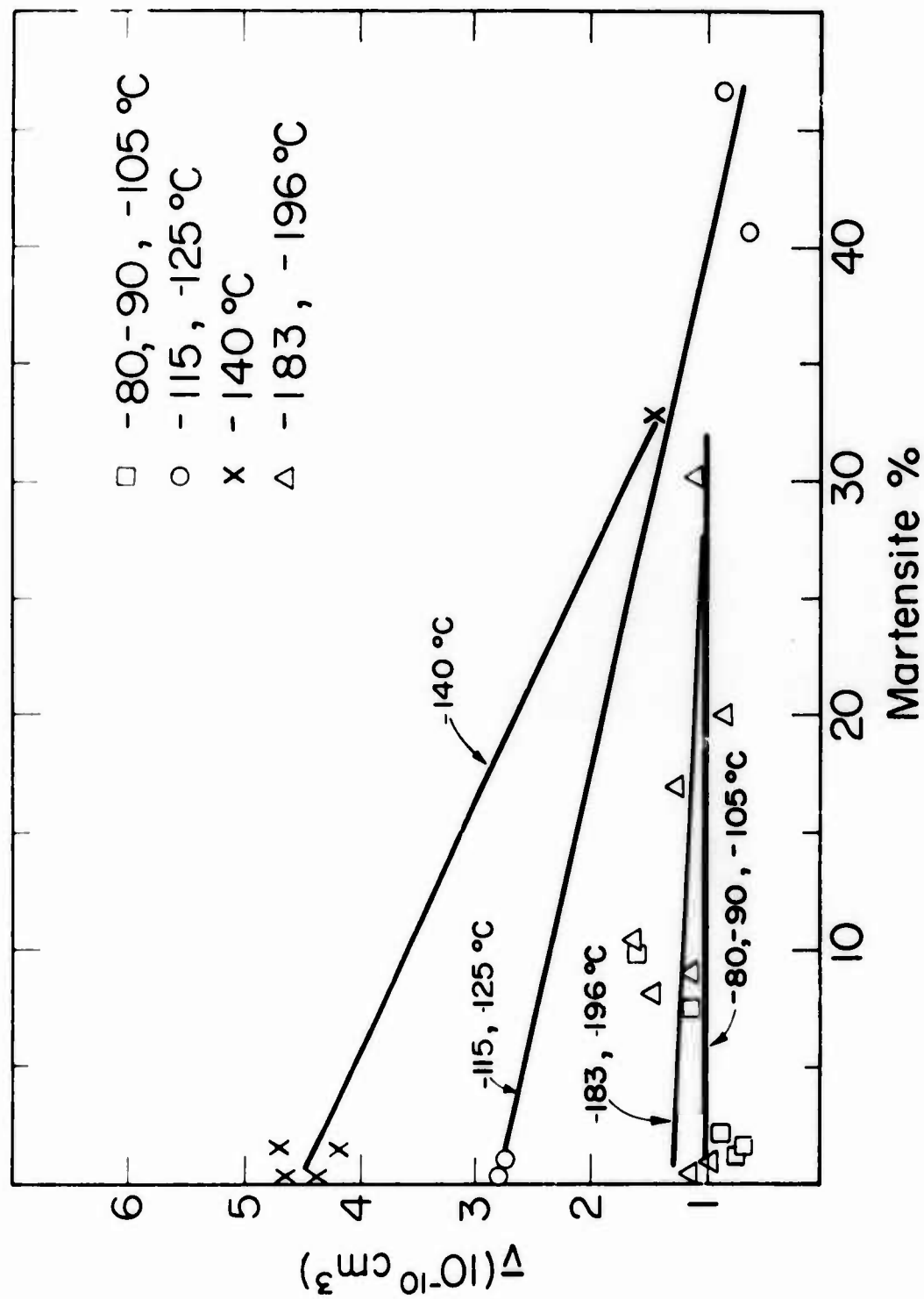


Fig.12 Mean plate volume \bar{v} , as a function of martensitic content, for Fe-24Ni-3Mn alloy at indicated temperatures⁽²⁴⁾.

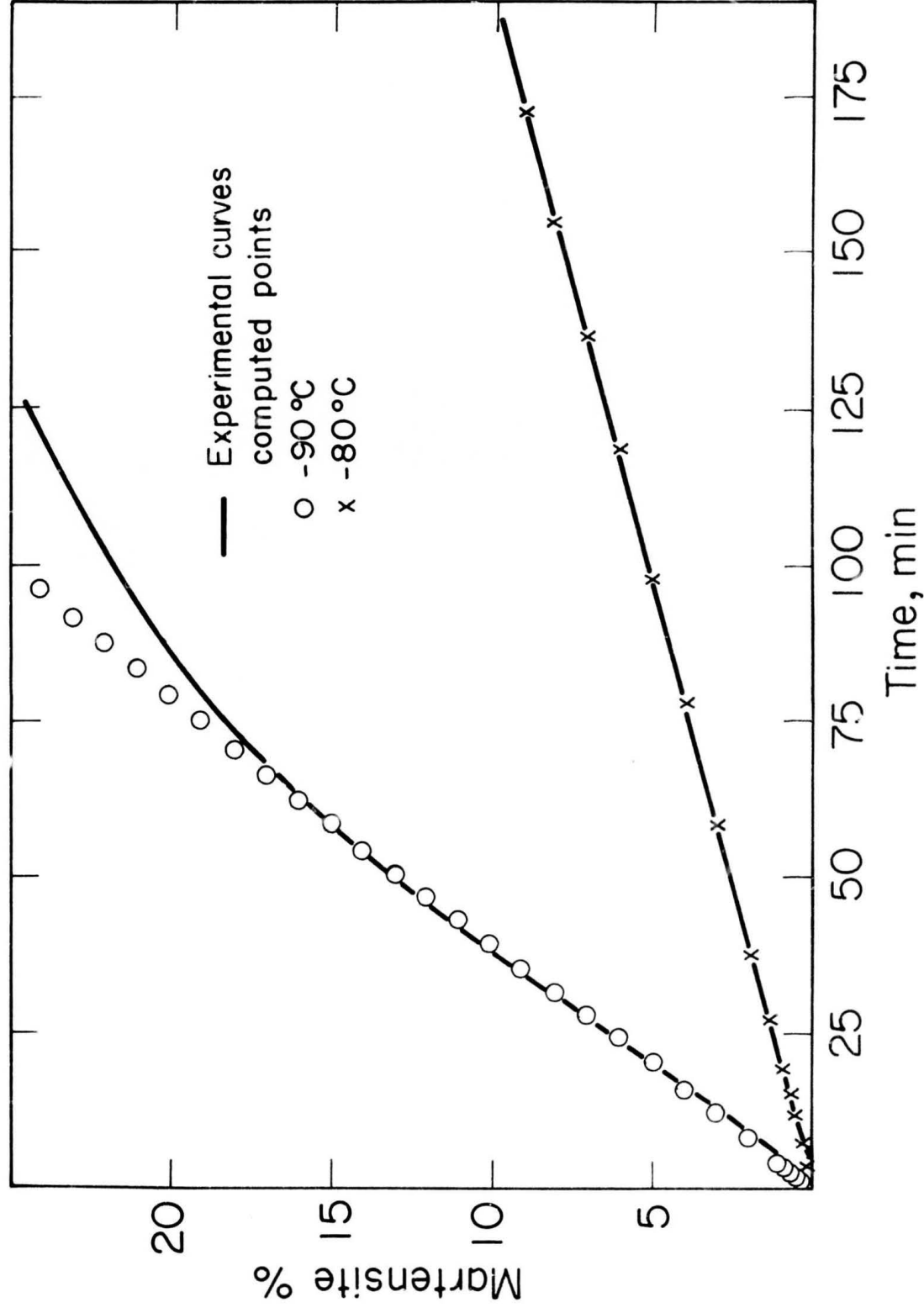


Fig. 13 Comparison of experimental transformation curves for Fe-24Ni-3Mn alloy with those computed from quantitative metallographic data⁽²⁴⁾.

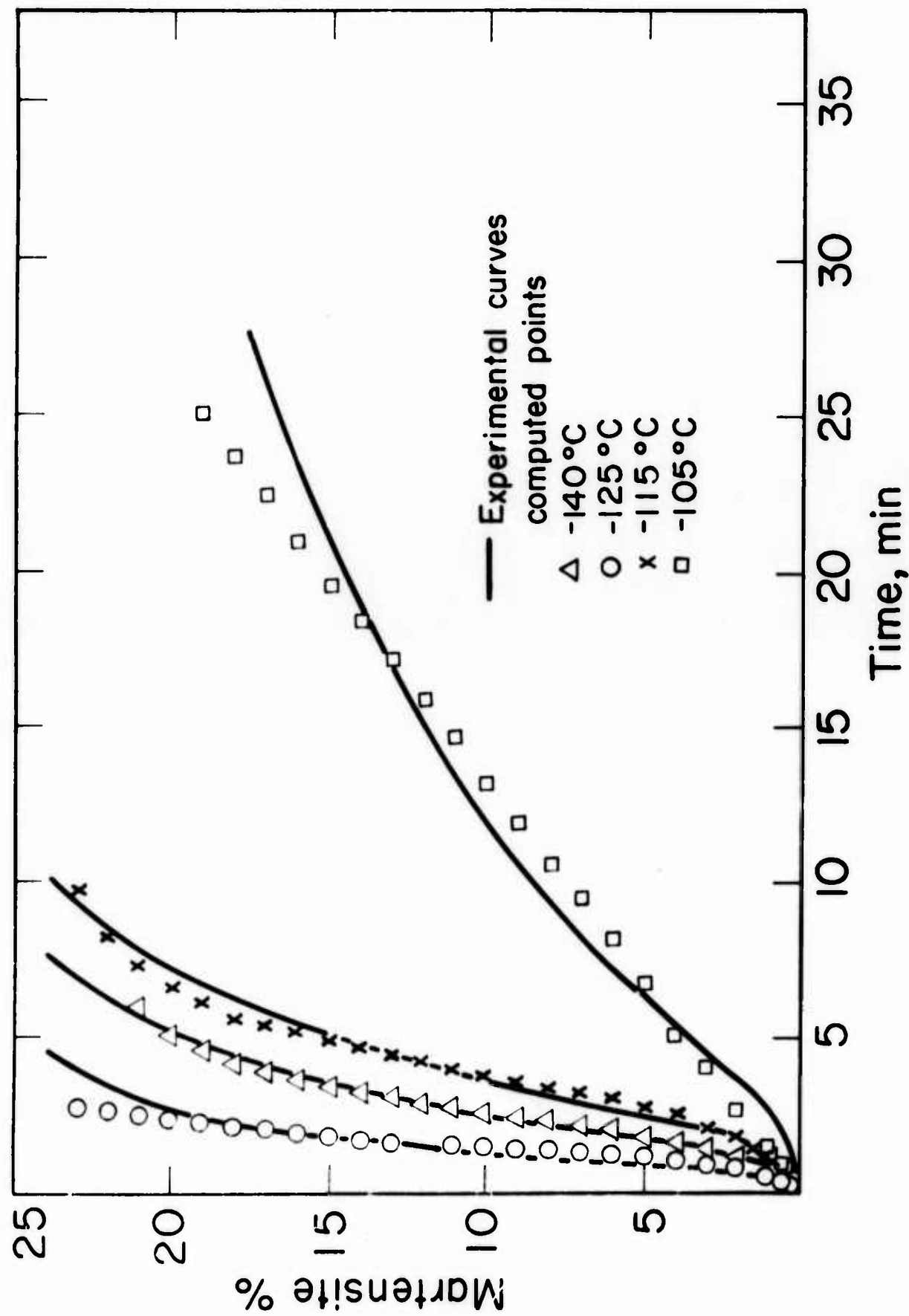


Fig. 14 Comparison of experimental transformation curves for Fe-24Ni-3Mn alloy with those computed from quantitative metallographic data⁽²⁴⁾.

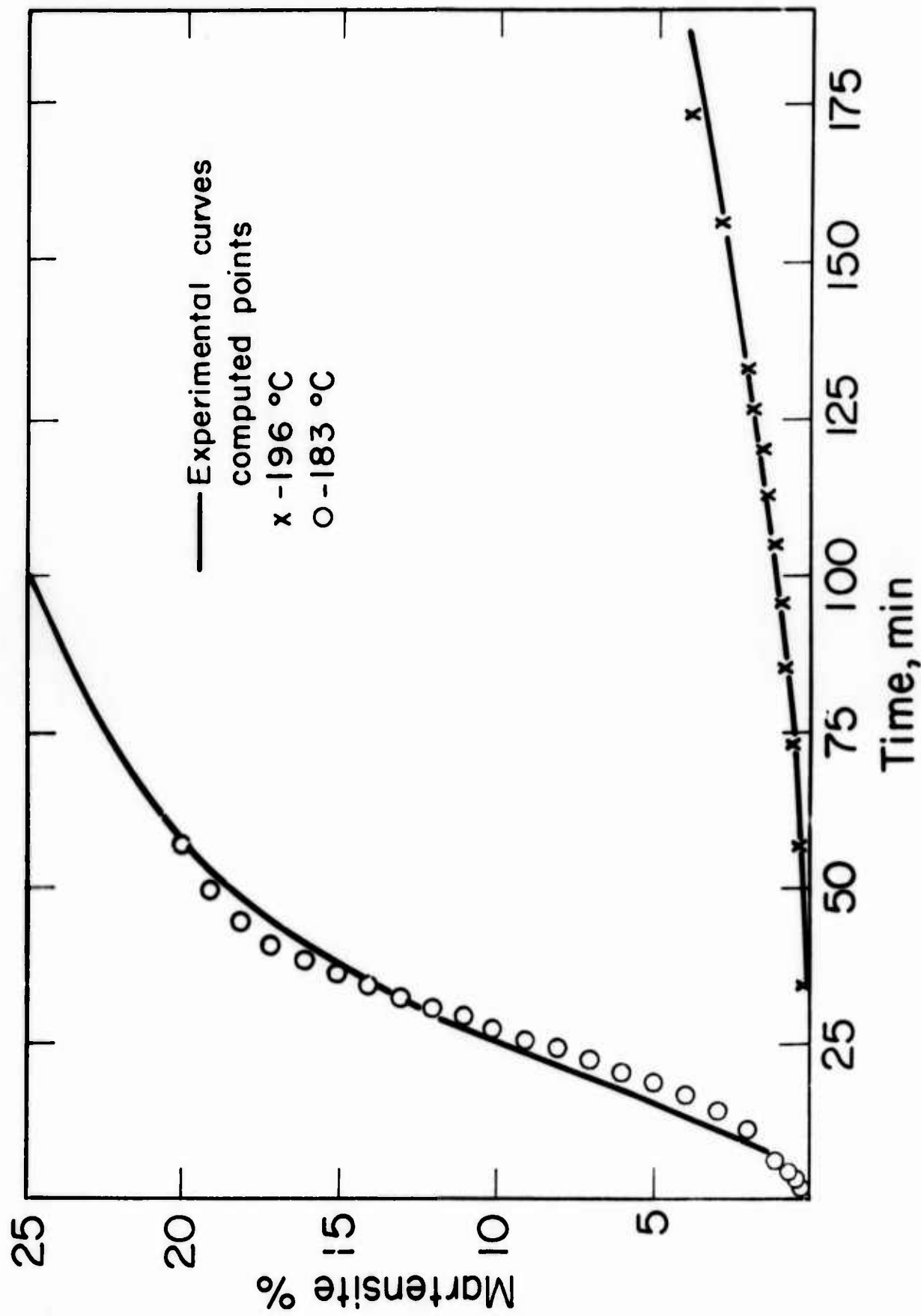


Fig. 15 Comparison of experimental transformation curves for Fe-24Ni-3Mn alloy with those computed from quantitative metallographic data⁽²⁴⁾.

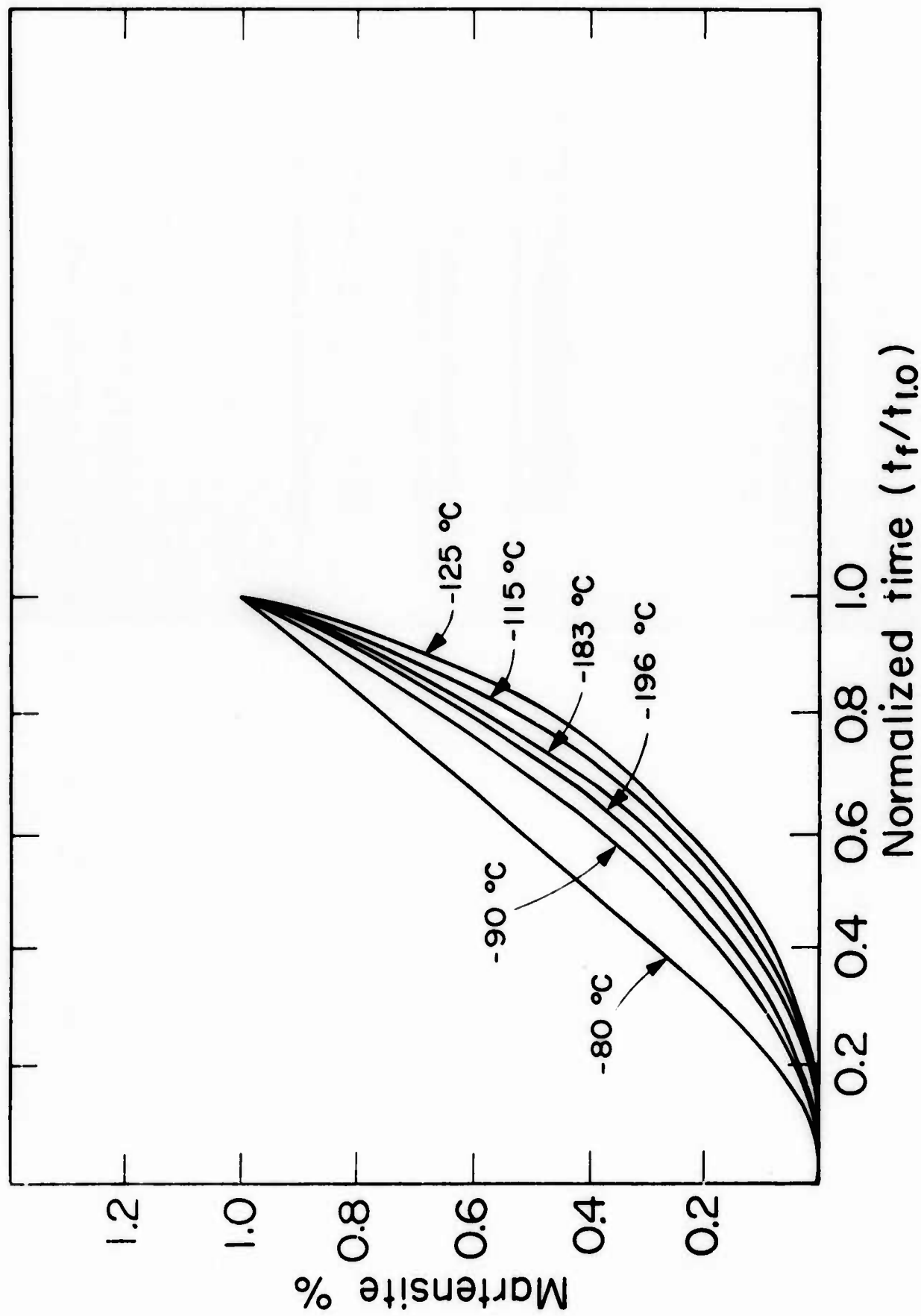


Fig. 16 Time-normalized transformation curves for Fe-24Ni-3Mn alloy showing the initial stages of the transformation at the indicated temperatures.

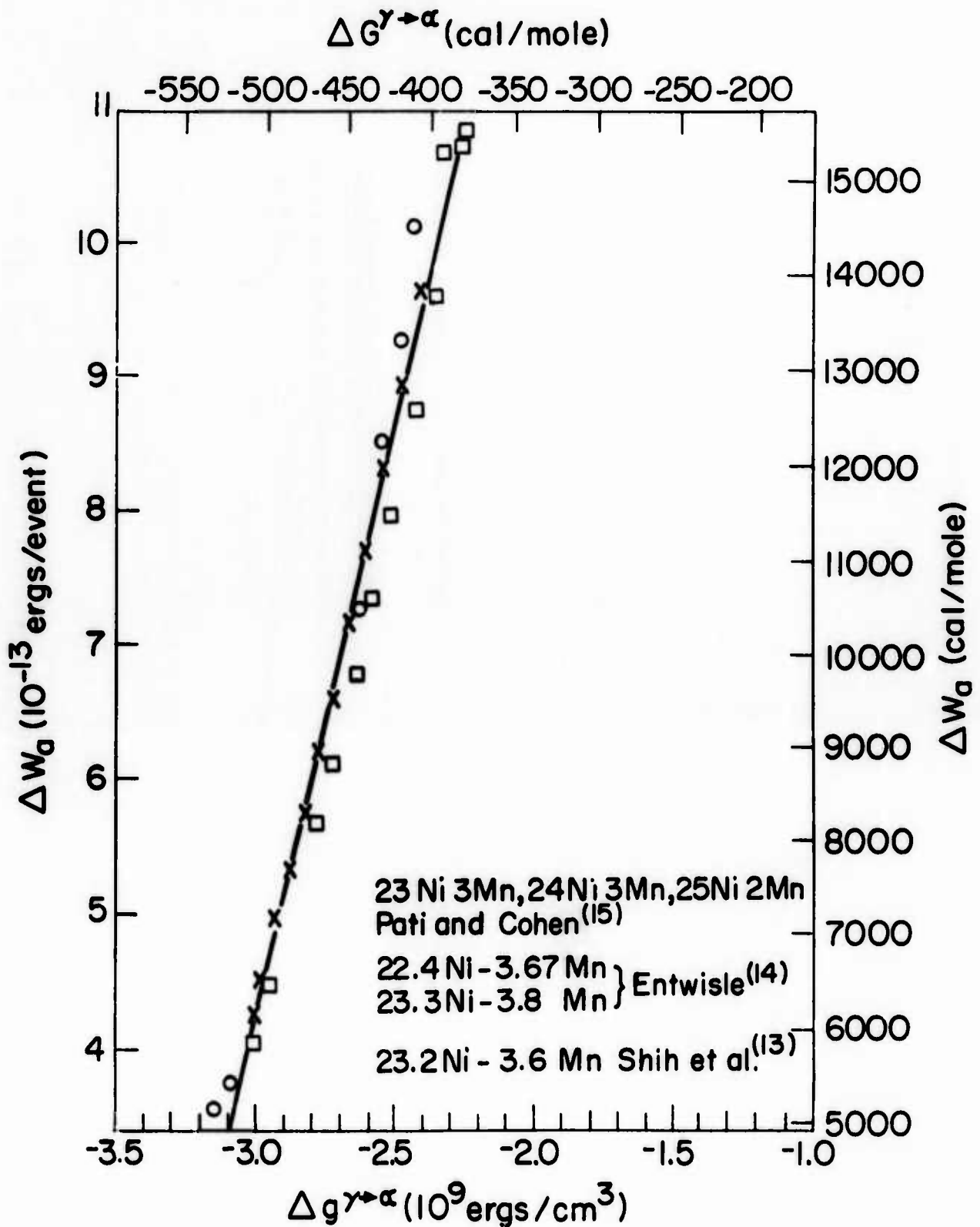


Fig.17 Measured activation energies for the isothermal martensitic transformation in Fe-Ni-Mn alloys as a function of free energy change accompanying the transformation⁽¹⁵⁾.

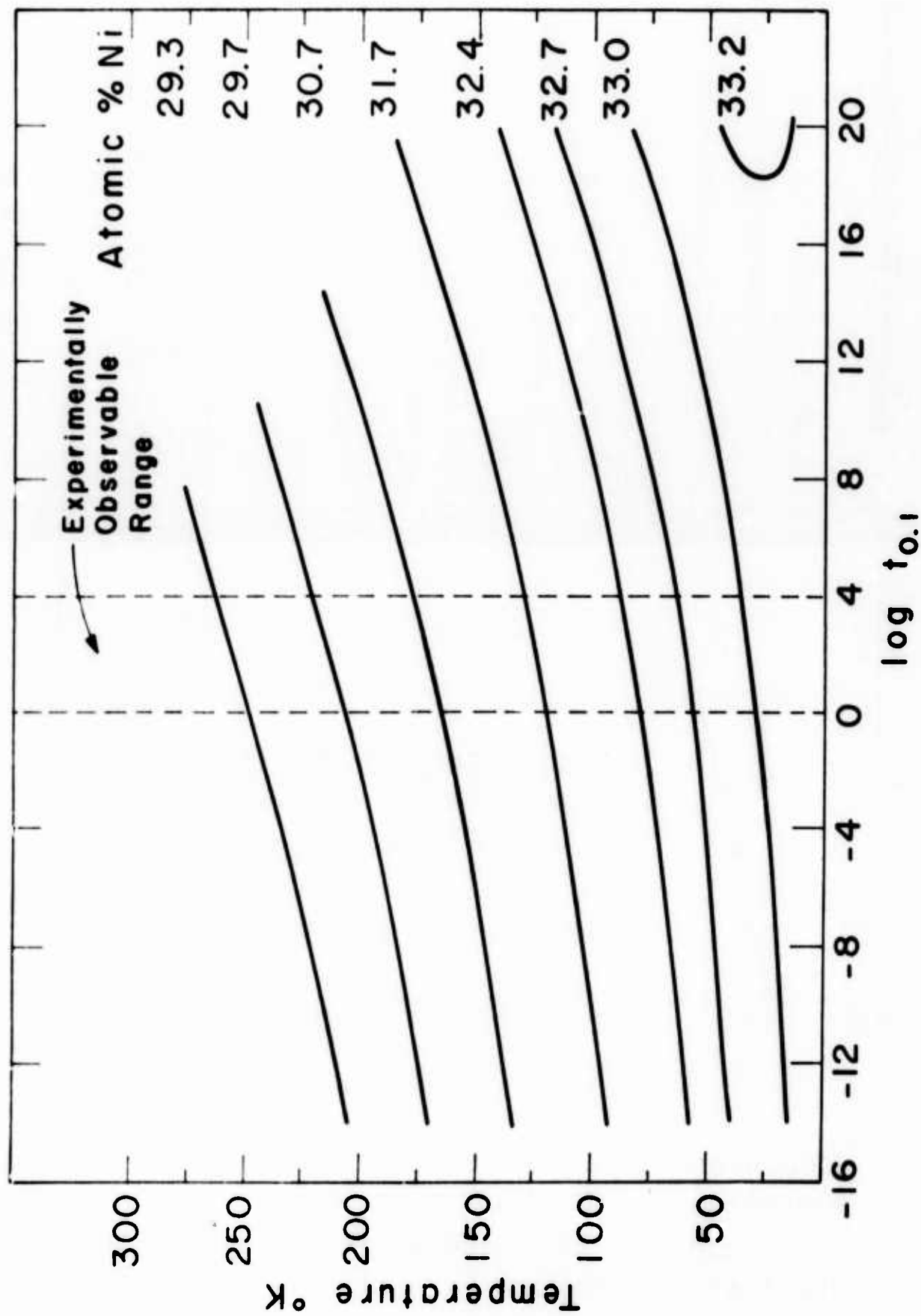


Fig. 18 Time for the initial 0.1% transformation ($t_{0.1}$) as a function of temperature and nickel content(3).